



# Electrochemical formation and characterization of Au nanostructures on a highly ordered pyrolytic graphite surface



José J. Arroyo Gómez<sup>a</sup>, Carolina Zubietá<sup>b</sup>, Ricardo M. Ferullo<sup>b</sup>, Silvana G. García<sup>a,\*</sup>

<sup>a</sup> Instituto de Ingeniería Electroquímica y Corrosión (INIEC), Departamento de Ingeniería Química, Universidad Nacional del Sur, Avda. Alem 1253, 8000 Bahía Blanca, Argentina

<sup>b</sup> INQUISUR, Departamento de Química, Universidad Nacional del Sur, Avda. Alem 1253, 8000 Bahía Blanca, Argentina

## ARTICLE INFO

### Article history:

Received 7 September 2015

Received in revised form 3 December 2015

Accepted 4 December 2015

Available online 10 December 2015

### Keywords:

Nanoparticles

Au

Electrodeposition

Highly ordered pyrolytic graphite

VASP

## ABSTRACT

The electrochemical formation of Au nanoparticles on a highly ordered pyrolytic graphite (HOPG) substrate using conventional electrochemical techniques and ex-situ AFM is reported. From the potentiostatic current transients studies, the Au electrodeposition process on HOPG surfaces was described, within the potential range considered, by a model involving instantaneous nucleation and diffusion controlled 3D growth, which was corroborated by the microscopic analysis. Initially, three-dimensional (3D) hemispherical nanoparticles distributed on surface defects (step edges) of the substrate were observed, with increasing particle size at more negative potentials. The double potential pulse technique allowed the formation of rounded deposits at low deposition potentials, which tend to form lines of nuclei aligned in defined directions leading to 3D ordered structures. By choosing suitable nucleation and growth pulses, one-dimensional (1D) deposits were possible, preferentially located on step edges of the HOPG substrate. Quantum-mechanical calculations confirmed the tendency of Au atoms to join selectively on surface defects, such as the HOPG step edges, at the early stages of Au electrodeposition.

© 2015 Elsevier B.V. All rights reserved.

## 1. Introduction

Metallic nanoparticles exhibit peculiar properties over bulk metal electrodes, being the catalytic activity one of the most important. Real and potential applications in devices such as sensors and fuel cells are based on these properties, which are primarily size and shape-dependent. It has been found that, among the noble metals, supported gold nanoparticles are an attractive material to be used as catalyst for several reactions, e.g. oxygen reduction [1,2] methanol oxidation [3], and CO oxidation [4]. The fact that the reactivity depends on both particles size and morphology makes an interesting task knowing the way gold particles nucleate and grow on different substrates.

Electrochemical deposition has been used as a reliable, versatile and low cost technique to produce metallic nanostructures [5] (from nanoparticles to nanowires) on different conducting surfaces. Nanocrystal size, density and surface texture can be controlled by potentiostatic pulses mode varying the deposition conditions. Carbon-based substrates have been generally used for the formation of gold nanostructures, mainly highly ordered pyrolytic

graphite (HOPG) [6–8] and glassy carbon (GC) [9,10]. These surfaces are the preferred supports for metallic nanoparticles due to their high overpotential for hydrogen evolution, their properties as inert and low-cost materials and the advantage to studying nucleation and growth processes neglecting the metal–metal interaction.

In this paper, we report new insights of the electrochemical formation of Au nanostructures (nanoparticles/nanowires) on HOPG using cyclic voltammetry and chronoamperometry. Current-time transients were performed in order to evaluate the nucleation mechanism. The generated Au crystals were characterized by ex-situ atomic force microscopy (AFM). As a complementary study, quantum-chemical calculations were carried out to analyze the interaction between Au atoms and a step edge on HOPG. Electronic information at the interface was extracted by analyzing the corresponding local density of states (LDOS).

## 2. Experimental and theoretical model

HOPG SPI-2 grade substrates (SPI Supplies, USA) were prepared by cleaving the surface with an adhesive tape immediately prior to each experiment. The electrode was held within a Teflon sheath that provided for the exposure of a  $0.216\text{ cm}^2$  area of the HOPG basal plane to the gold plating solution using a Teflon O-ring.

\* Corresponding author. Tel./fax: +54 291 4595182.

E-mail address: [sgarcia@criba.edu.ar](mailto:sgarcia@criba.edu.ar) (S.G. García).

The electrodeposition of the Au nanoparticles on HOPG was performed from a 1 mM  $\text{AuHCl}_4 + 0.16 \text{ M H}_2\text{SO}_4$  solution, prepared from suprapure chemicals (E. Merck, Darmstadt) and tri-distilled water. The electrochemical experiments were carried out at a temperature of 298 K using a conventional three-electrode electrochemical cell. The electrolyte was deareated by bubbling purified nitrogen prior to each experiment. The counter electrode was a Pt sheet ( $1 \text{ cm}^2$ ) and the reference electrode was a  $\text{Hg}/\text{Hg}_2\text{SO}_4/\text{K}_2\text{SO}_4$  saturated electrode, SSE ( $E_{\text{SSE}} = 0.658 \text{ V}$  vs. SHE). All electrode potentials are referred to the SSE.

Cyclic voltammetry and chronoamperometry experiments were performed using a computer-controlled EG&G Princeton Applied Research model 273A potentiostat–galvanostat.

The morphology and size of the electrodeposited Au nanoparticles were characterized by ex-situ AFM, using a standard Nanoscope III microscope (Digital Instruments, Santa Barbara, USA) operated in contact mode. A scanner of  $15 \mu\text{m}$ , and oxide-sharpened silicon nitride probes (Veeco probes) with a nominal tip-radius between 5–40 nm and spring constant of  $0.06 \text{ N m}^{-1}$  were used.

Quantum-Chemical calculations were carried out in order to simulate the growth of Au particles on a graphite step edge using a slab model by means of the Vienna Ab-initio Simulation Package (VASP) [11–13], which solves the Kohn–Sham equation of the density functional theory (DFT) using a plane wave basis set. A good convergence was achieved with a cut-off energy of 450 eV for the kinetic energy. The projector augmented wave (PAW) method was used to describe the effect of the core electrons on the valence states. The exchange and correlation effects were calculated by the PBE functional [14]. The graphite surface was represented by only one sheet which is constructed by means of a  $6 \times 1$  supercell with 24 carbon atoms and a gap of  $20 \text{ \AA}$  in the normal direction to the surface. The two dimensional Brillouin integrations were performed on a grid of  $3 \times 9 \times 1$  Monkhorst-Pack special k-points and all the calculations were carried out at the spin-polarized level. Optimized geometries were found when the forces on atoms were smaller than  $0.01 \text{ eV}/\text{\AA}$ . A large box of  $20 \times 20 \times 20 \text{ \AA}$  was used to obtain the gas-phase atomic Au energy. The electronic structure of the  $\text{Au}_n/\text{graphene}$  system was evaluated from Bader charges and local density of states (LDOS) curves.

### 3. Results and discussion

#### 3.1. Substrate characterization

Previous to the Au nanoparticles formation, the surface of the substrate was examined and characterized using ex-situ AFM (Fig. 1). The HOPG surface consists of flat terraces separated by monoatomic step edges and very few other superficial defects (Fig. 1). This type of HOPG (SPI-2) presents domains of approximately linear step edges that are oriented parallel with one another, suitable for the fabrication of metal nanowires by the ESED (Electrochemical Step Edge Decoration) method [15].

The voltammetric data revealed that the substrate immersed in  $0.5 \text{ M H}_2\text{SO}_4$ , blank solution, showed no faradaic phenomena in the potential range where the Au deposition-dissolution processes take place, i.e.  $-0.3 \leq E/\text{V} \leq 1.0$  (data not shown).

#### 3.2. Electrodeposition of Au particles

##### 3.2.1. Voltammetric response

Cyclic voltammetry was utilized to obtain brief information of the Au electrodeposition on HOPG electrodes in the 1 mM  $\text{AuHCl}_4 + 0.16 \text{ M H}_2\text{SO}_4$  plating solution. The voltammetric measurements were obtained in the potential range  $-0.3 \leq E/\text{V} \leq 1.0$

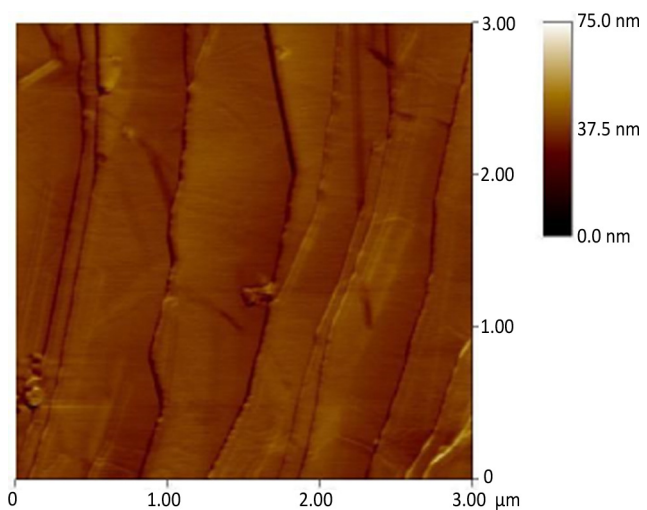


**Fig. 1.** AFM image of the HOPG. Scan size  $3 \mu\text{m} \times 3 \mu\text{m}$ .

and the scan was initiated at  $\approx 0.7 \text{ V}$ . Fig. 2 shows the typical voltammogram of this system, recorded at  $|dE/dt| = 10 \text{ mV/s}$ .

During the cathodic sweep, at potentials close to  $E = 0.0 \text{ V}$ , the reduction current density peak of the gold species is observed. The hysteresis evidenced during the anodic sweep indicates that the Au nucleation on HOPG has a behavior of a slow nucleation and 3D growth process controlled by diffusion [16,17]. The well-defined current density peak that appears close to  $E \approx 0.7 \text{ V}$  is related to the oxidation of Au deposits.

##### 3.2.2. Chronoamperometric analysis

As indicated previously, the properties of nanoparticles depend on their size and shape, and therefore, it is important to understand the formation mechanisms of such nanocrystals to achieve a good control of their morphology.

The nucleation process of Au onto HOPG was studied using the potential step technique. Fig. 3 shows several potentiostatic current transients recorded from an initial potential value of  $\sim 0.6 \text{ V}$ , where no Au is deposited on the electrode surface, to a final potentials,  $E$ , varying between  $-0.03 \text{ V}$  and  $0.09 \text{ V}$ . The chronoamperometric curves exhibit the typical behavior of 3D nucleation process and growth controlled by diffusion of the electroactive species [16].

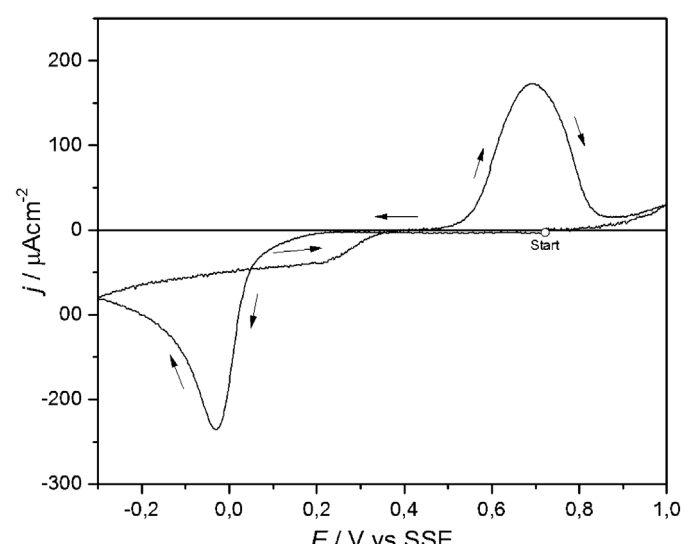


**Fig. 2.** Cyclic voltammogram of the system HOPG/1 mM  $\text{AuHCl}_4 + 0.16 \text{ M H}_2\text{SO}_4$ ,  $|dE/dt| = 10 \text{ mV/s}$ .

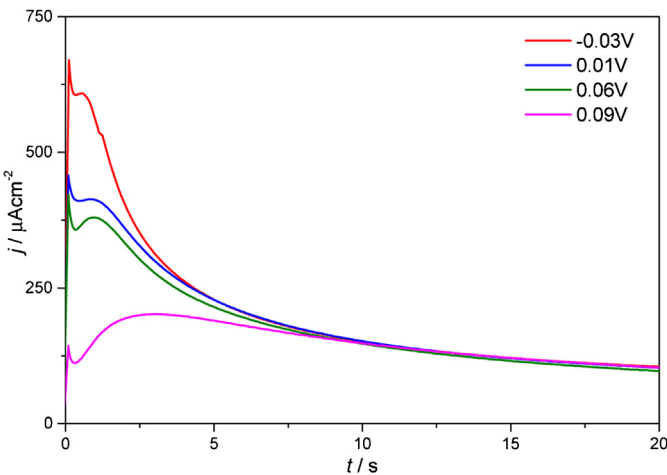


**Fig. 3.** Family of potentiostatic current transients for the nucleation of Au on HOPG from 1 mM AuHCl<sub>4</sub> + 0.16 M H<sub>2</sub>SO<sub>4</sub> solution.

After a sharp current density peak at very short times related to the electrochemical double-layer charging, an increase in current density is observed due to the formation and growth of discrete nuclei. After these stages of the nucleation process, the individual diffusion zones of adjacent nuclei overlap, and the current density reaches a maximum value  $j_m$  at the time  $t_m$  and then, decays following the usual  $t^{-1/2}$  dependence according to the Cottrell equation [9,17]. When the deposition potential is made more negative,  $j_m$  increases gradually whereas  $t_m$  shifts slightly to smaller values.

On the other hand, the non-dimensional plots  $(j/j_{max})^2$  vs  $(t/t_{max})$ , proposed by Scharifker and Hills [18] are widely used for the determination of nucleation and growth mechanisms by comparing the experimental results with the theoretical dimensionless transients for the limiting cases of instantaneous and progressive nucleation, generated by Eqs. (1) and (2):

$$\left(\frac{j}{j_{max}}\right)^2 = 1.9542 \left\{ 1 - \exp \left[ -1.2564 \left( \frac{t}{t_{max}} \right) \right] \right\}^2 \left( \frac{t}{t_{max}} \right)^{-1} \quad (1)$$

$$\left(\frac{j}{j_{max}}\right)^2 = 1.2254 \left\{ 1 - \exp \left[ -2.3367 \left( \frac{t}{t_{max}} \right) \right] \right\}^2 \left( \frac{t}{t_{max}} \right)^{-1} \quad (2)$$

**Fig. 4** shows the comparison of the experimental data of various current transients for the Au/HOPG system reported in **Fig. 3**, along

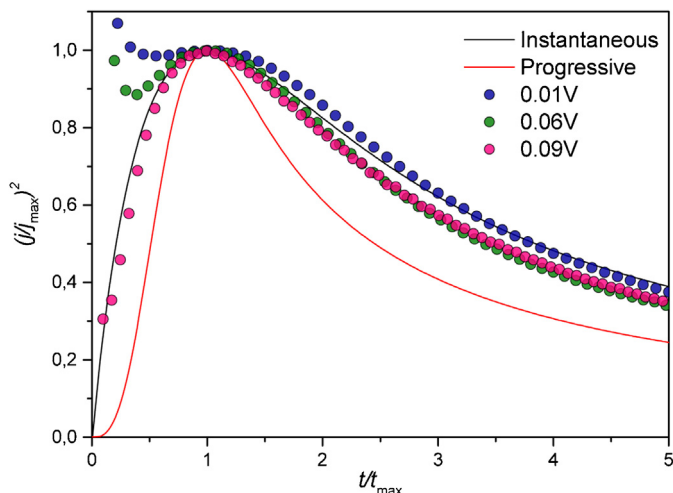


**Fig. 4.** Comparison of theoretical non-dimensional plots for the instantaneous and progressive nucleation with experimental current transients showed in **Fig. 3** for the Au electrodeposition on HOPG.

with the theoretical curves for the limiting cases of instantaneous and progressive nucleation.

In the Au/HOPG system the gold nucleation tends to follow the response predicted for a 3D instantaneous nucleation, where all the nuclei are formed as soon as the potential pulse is applied.

### 3.2.3. Morphologic analysis

The Au deposits on HOPG were characterized employing ex-situ AFM. **Fig. 5** illustrates AFM images of Au nanostructures on HOPG after applying a potential pulse from an initial potential  $E_i = 0.45$  V to  $E = -0.20$  V (**Fig. 5a**) and to  $E = -0.35$  V (**Fig. 5b**) during 20 s.

The AFM image in **Fig. 5a** shows 3D hemispherical-shaped deposits on HOPG with an average size of 160 nm, which are mainly distributed on the step edges of the substrate, acting as active sites for the metal nucleation. The relatively uniform size of these nanocrystals tends to follow an instantaneous nucleation mechanism as it has been demonstrated previously from chronoamperometric results. The covered area of Au deposits was estimated at 0.0173 cm<sup>2</sup>, corresponding to 8% of the geometric area of the HOPG substrate (statistical value based on measurements from several AFM images of different regions of the electrode). At more negative potentials,  $E = -0.35$  V, the AFM image (**Fig. 5b**) shows the presence of Au deposits, some of them with hexagonal shape and slightly larger dimensions, as can be seen in the size distributions, while others begin to coalesce leading to larger nanoparticles. The covered area of Au deposits was found to be 0.0509 cm<sup>2</sup>, corresponding to 23.56% of the HOPG geometric area. As can be seen in **Fig. 5**, the increase in the final potential of the applied pulse to more negative values, gives different nanocrystals shapes due to the change in diffusion and growth mechanisms of the gold atoms on the substrate [16].

Using the simple potential pulse technique, the electrodeposited Au nanoparticles present a broad size distribution caused by a phenomena called “interparticle diffusion coupling” (IDC) described by Penner [15], which leads to a dispersion in the growth rates of each individual particle. The effect of IDC can be reduced using the double potential pulse technique by which the nucleation and growth processes can be controlled independently. This technique consists in applying a nucleation pulse for very short times, in which the first nuclei are formed, followed by a growth pulse in which the probabilities of new nuclei generation are practically zero. With this methodology it has been possible to obtain uniform sized clusters, aligned at step edges of the HOPG surface.

In **Fig. 6**, the formation of one-dimensional structures (nanowires), obtained using a simple potential pulse of  $E = 0.0$  V during 5 s (a) and a double potential pulse with a nucleation potential,  $E_N = -0.3$  V during 10 ms and a growth potential  $E_G = 0.4$  V during 100 s (b), is observed. The diameter of the Au structures shown in **Fig. 6a** is about 200 nm with a height of up to 20 nm. The diameter of the uni-dimensional structures generated by double pulse, which present the tendency to form more continuous and longer nuclei lines, ranges between 75 nm and 180 nm, with an average height of 10 nm. The covered area of Au crystallites obtained by simple and double pulse was estimated at 0.0171 cm<sup>2</sup> and 0.0263 cm<sup>2</sup>, corresponding to 7.92% and 12.17% of the HOPG geometric area, respectively.

### 3.3. Theoretical calculations

Theoretical calculations were performed on the Au/HOPG system in order to analyze the one-dimensional Au nanostructures observed on the substrate step edges in AFM images (c.f. **Fig. 6**). The edge of a monoatomic step on graphite was simulated by adding a chain of condensed aromatic rings over a graphene layer, as illustrated in **Fig. 7**. The dangling bonds belonging of one of

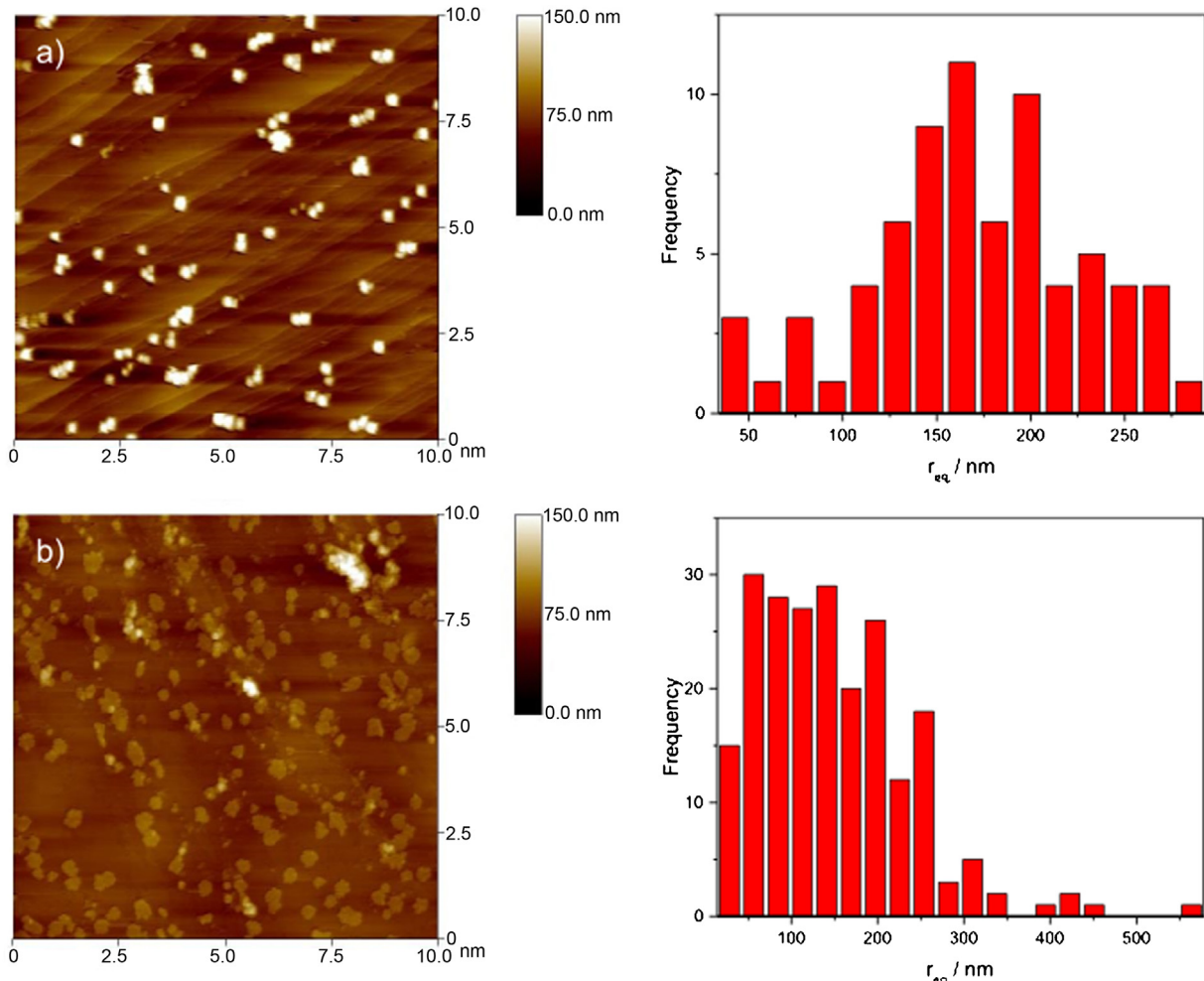


**Fig. 5.** Gold deposits onto HOPG using the single pulse technique, with its size distribution, from  $E_i = 0.45$  V to (a)  $E = 0.05$  V and (b)  $E = -0.35$  V, during 20 s.

the sides was saturated with hydrogen atoms to represent the continuity of the carbon layer. All the C and H atoms of the chain and Au atoms were allowed to relax during optimization calculations. Most of the commonly used DFT based methods rely on approximations to the electron exchange and correlation which do not properly describe the long-range van der Waals forces, such as the one present between graphite layers. For this reason,

an empirical correction was used consisting in the addition of a damped atom-pairwise dispersion term [19].

Here we consider an ideal “atom by atom” nucleation process. In that, Au atoms firstly interact with the unsaturated C atoms of the edge step. Once this step is fully covered by Au, the metal structure grows by the addition of subsequent Au atoms until taking six Au atoms per supercell. It is clear that this model is

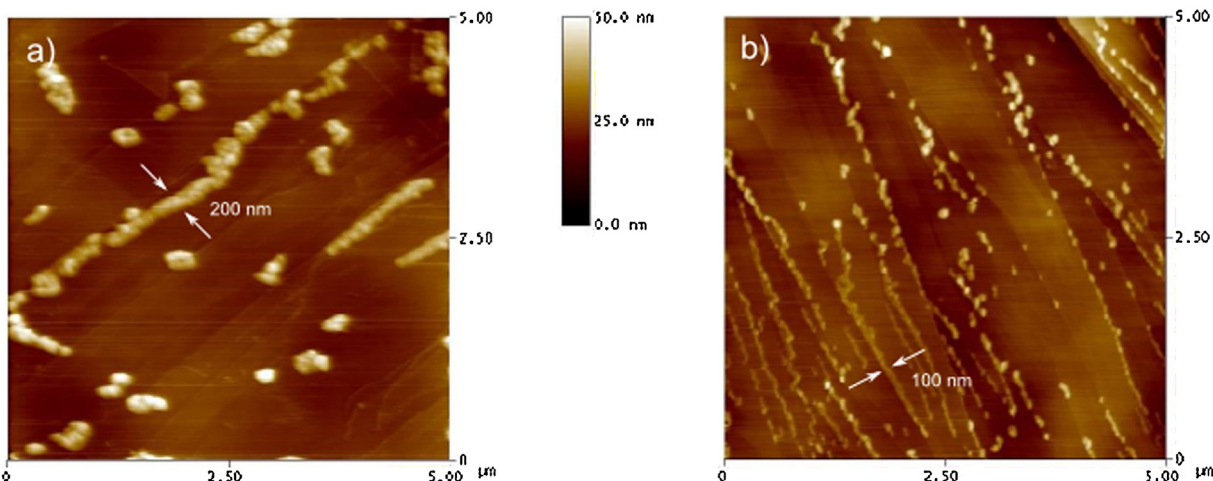


**Fig. 6.** Gold nanowires formation on HOPG using the simple (a) and double (b) pulse technique.

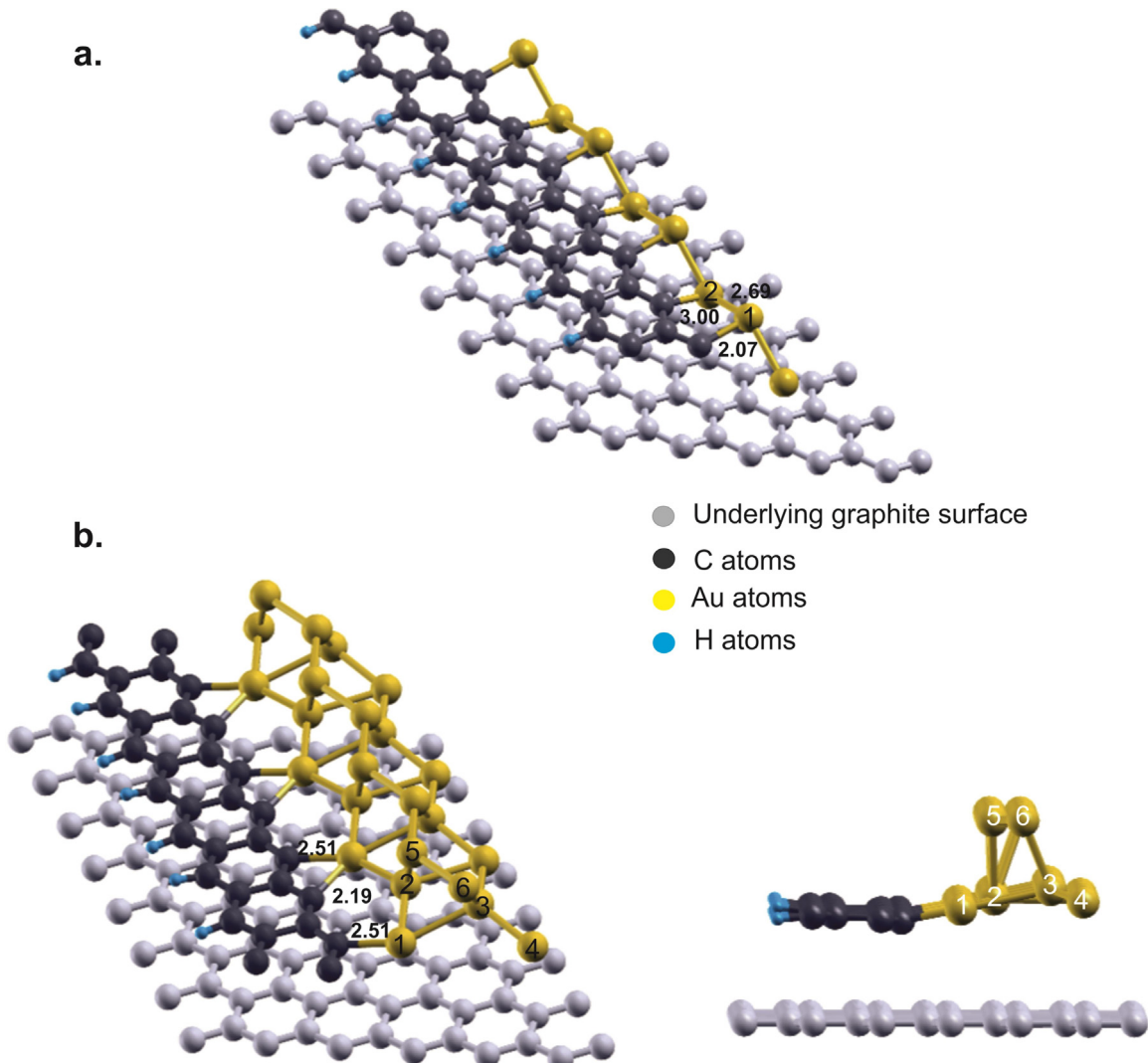


**Fig. 7.** (a) Optimized geometry of the zig-zag monoatomic Au chain on stepped graphite (two Au atoms per cell); (b) Two views of the one-dimensional Au structure grown along the graphite step edge (six Au atoms per cell). Distances are expressed in Å.

far from representing the experimentally obtained metallic structures, in particular with respect to their size. However, this type of first principle methods (based on quantum mechanics postulates) provides a very valuable electronic structure description at a fundamental level, as we shall see later. The energy associated with this ideal process is calculated by the difference between the Au/graphite energy and the sum of the energies of the separated fragments (carbon substrate and Au atom at gas phase). Thus, for the primary interaction between the first Au atom and the stepped graphite supercell we can define the interaction energy as:

$$\Delta E = E(\text{Au}/\text{stepped graphite}) - E(\text{stepped graphite}) - E(\text{Au}) \quad (3)$$

According with that, negative values correspond to exothermic processes. Computed values of  $\Delta E$  show a strong binding when the first Au atom interacts with the unsaturated C atoms of the stepped graphite surface, with  $\Delta E = -3.30$  eV. To obtain a larger metal aggregate, subsequent incoming Au atoms must interact with the carbon substrate and among themselves and consequently the structure grows. The energy difference is now defined as the energy related to the formation of one Au particle when an atom in gas

phase adds to a metal pre-adsorbed particle,

$$\begin{aligned} \Delta E &= E(\text{Au}_n/\text{stepped graphite}) - E(\text{Au}_{n-1}/\text{stepped graphite}) \\ &\quad - E(\text{Au}) \end{aligned} \quad (4)$$

The addition of the second Au atom is very strong with a  $\Delta E$  value similar than that of the first Au atom ( $-3.15$  eV). With this second Au atom per cell, a very stable zig-zag monoatomic chain of Au is formed, as it can be seen in Fig. 7a, where the different Au atoms are identified with numbers. For a better observation of the geometry, the C atoms of the outer layer are shown in black. In the same figure, the Au-C and Au-Au distances are indicated as well. Fig. 7a represents an ideal intermediate structure from which the Au aggregate begins to grow along the graphite edge.

In the following sequence, from  $n=3$  to  $n=6$ , subsequent Au atoms interact weaker with the substrate,  $\Delta E$  presenting an average value of approximately  $-2.1$  eV. Therefore, the interaction of Au with the edge step is much stronger than the Au-Au coupling. Besides, the deposition of Au on steps is energetically preferred than on the flat surface; indeed, DFT calculations performed on the adsorption of Au atoms on graphene sheets show adsorption

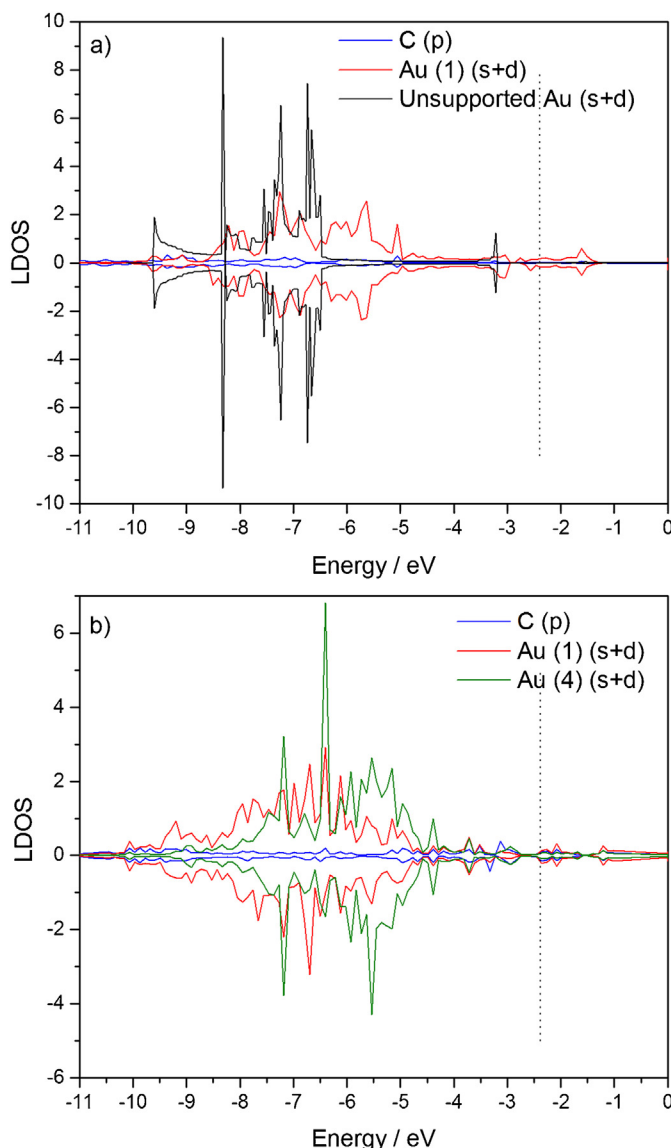


**Fig. 8.** (a) LDOS of Au atoms for supported and unsupported monoatomic zig-zag chains (two Au atoms per cell); (b) LDOS of two different Au atoms corresponding to the one-dimensional Au structure (six atoms per cell). LDOS for C atoms directly linked with Au(1) are also shown. The vertical dotted line corresponds to the Fermi level. Positive values refer to spin up states and negative values to spin down states.

energy values ranging between  $-0.3$  and  $-0.9$  eV, depending on the approximation used to simulate dispersion forces [20].

In Fig. 7b, the optimized geometry of Au grown on stepped graphite is showed (with six Au atoms per cell). The calculated Au–Au distance falls in the range between 2.65 and 2.90 Å. It can be seen that Au structure grows from the graphite edge, being the interaction very weak between Au and the underlying carbon layer.

When the metal monoatomic chain is formed along the edge (Fig. 7a) both Au atoms acquire positive charge (0.08 and 0.12e for Au(1) and Au(2), respectively), indicating an electronic charge transfer from the metal aggregate to the substrate. For the larger metal structure (Fig. 7b), calculations show that it has a total charge of only 0.04e. In this case, Au(1) and Au(2) atoms are positively charged (0.16 and 0.05e, respectively) as well, while Au(6) remains neutral; Au(3), Au(4) and Au(5) atoms acquire a charge of  $-0.04$ ,  $-0.11$  and  $-0.02$ e, respectively. Consequently, the Au structure tends to polarize toward the outermost metal atoms. The C atom

directly linked to Au(1) presents a net charge of  $-0.16$ e indicating a certain degree of ionic character at the Au-C interface.

In Fig. 8, the LDOS profiles for Au/graphene system are presented. Fig. 8a shows the corresponding curves for the Au(1) atom related to the supported Au monoatomic zig-zag chain, and to the edge C atom which is linked with. For comparison, the corresponding LDOS profile for a Au atom of an isolated monoatomic chain is also represented; in this case, the geometry is taken from the optimized supported structure. It is clear that the Au (s+d) states disperse energetically with respect to non-interacting Au in order to overlap with the C (p) states. Indeed, it can be observed that Au(1)-C interaction occurs in a wide energetic range (between  $-3$  and  $-10$  eV), suggesting the formation of a covalent bond by hybridization between Au (s+d) and C (p) orbitals.

In Fig. 8b, the LDOS profile for the large Au aggregate (six Au atoms per cell, Fig. 7b) is plotted. The curves correspond to a C atom of the step and to two different Au atoms, namely, the nearest one to that C, Au(1), and the Au atom with the highest negative charge, Au(4). As expected, also in this case the Au(1)-C interaction occurs in a wide energetic range. For Au(4) a shift to higher energy values takes place; indeed, the corresponding LDOS increases within the zone between  $-5$  and  $-6$  eV, and decreases between  $-8$  and  $-10$  eV with respect to the states of Au(1). The relative position of the Au(4) band is compatible with a negatively charged atom, in agreement with the charge values above mentioned. Furthermore, the Au structure presents a small net magnetization, of around 0.02 Bohr magnetons per cell.

#### 4. Conclusions

In this work, the electrochemical formation of Au nanoparticles on a HOPG substrate from 1 mM  $\text{AuHCl}_4 + 0.16$  M  $\text{H}_2\text{SO}_4$  plating solution was studied. The analysis of current density transients have shown that the Au electrodeposition is a diffusion-controlled process with a typical 3D nucleation mechanism on HOPG electrodes. The gold nucleation mechanism tends to follow the response predicted for a 3D instantaneous nucleation in the potential range considered. By choosing suitable nucleation and growth pulses, long and continuous one-dimensional Au deposits (nanowires) were possible, preferentially located on step edges of the HOPG substrate.

DFT simulations confirm the tendency of Au atoms to group over the edge steps of the substrate, at the early stages of Au electrodeposition. Calculations indicate that the strong Au-C bonds at the interface are mainly of covalent nature with a rather small contribution of ionic character.

#### Acknowledgments

The authors wish to thank the Universidad Nacional del Sur, Argentina, for the financial support of this work. J.J. Arroyo Gómez acknowledges a fellowship granted by CONICET.

#### References

- [1] G. Vazquez-Huerta, G. Ramos-Sánchez, A. Rodriguez-Castellanos, D. Meza-Calderon, R. Antaño-López, O. Solorza-Feria, Electrochemical analysis of the kinetics and mechanism of the oxygen reduction reaction on Au nanoparticles, *J. Electroanal. Chem.* 645 (2010) 35.
- [2] M. El-Deab, T. Sotomura, T. Ohsaka, Oxygen reduction at Au nanoparticles electrodeposited on different carbon substrates, *Electrochim. Acta* 52 (2006) 1792–1798.
- [3] S. Yan, S. Zhang, Y. Lin, G. Liu, Electrocatalytic performance of gold nanoparticles supported on activated carbon for methanol oxidation in alkaline solution, *J. Phys. Chem. C* 115 (2011) 6986–6993.

- [4] P. Diao, D.F. Zhang, M. Guo, Q. Zhang, Electrocatalytic oxidation of CO on supported gold nanoparticles and submicroparticles: Support and size effects in electrochemical systems, *J. Catal.* 250 (2007) 247–253.
- [5] E.C. Walter, M.P. Zach, F. Favier, B.J. Murray, K. Inazu, J.C. Hemminger, R.M. Penner, Metal nanowires arrays by electrodeposition, *ChemPhysChem* 4 (2003) 131–138.
- [6] H. Martin, P. Carro, A. Hernández Creus, S. González, G. Andreasen, R.C. Salvarezza, A.J. Arvia, The influence of adsorbates on the growth mode of gold islands electrodeposited on the basal plane of graphite, *Langmuir* 16 (2000) 2915–2923.
- [7] T. Jing, W. Jiang-Ming, X. Zhao-Xiong, M. Bing-Wei, Electrochemical preparation and AFM characterization of gold nanoparticles on HOPG, *J. Chin. Electr. Microsc. Soc.* 20 (2001) 599–602.
- [8] T. Brüllé, W. Ju, P. Niedermayr, A. Denisenko, O. Paschos, O. Schneider, U. Stimming, Size-dependent electrocatalytic activity of gold nanoparticles on HOPG and highly boron-doped diamond surfaces, *Molecules* 16 (2011) 10059–10077.
- [9] L. Komsitska, G. Staikov, Electrocrystallization of Au nanoparticles on glassy carbon from  $\text{HClO}_4$  solution containing  $[\text{AuCl}_4]^-$ , *Electrochim. Acta* 54 (2008) 168–172.
- [10] T.H. Lin, W.H. Hung, Electrochemical deposition of gold nanoparticles on a glassy carbon electrode modified with sulfanilic acid, *J. Electrochem. Soc.* 156 (2009) D45–D50.
- [11] G. Kresse, J. Hafner, *Ab initio* molecular dynamics for liquid metals, *Phys. Rev. B* 47 (1993) 558–561.
- [12] G. Kresse, J. Hafner, *Ab initio* molecular dynamics for open-shell transition metals, *Phys. Rev. B* 48 (1993) 13115–13118.
- [13] G. Kresse, J. Hafner, *Ab initio* molecular-dynamics simulation of the liquid–metal–amorphous–semiconductor transition in germanium, *Phys. Rev. B* 49 (1994) 14251–14269.
- [14] J.P. Perdew, K. Burke, M. Ernzerhof, Generalized gradient approximation made simple, *Phys. Rev. Lett.* 77 (1996) 3865–3868.
- [15] R.M. Penner, Mesoscopic metal particles and wires by electrodeposition, *J. Phys. Chem. B* 106 (2002) 3339–3353.
- [16] H. Martin, P. Carro, A. Hernández Creus, S. González, R.C. Salvarezza, A.J. Arvia, Growth mode transition involving a potential-dependent atom diffusion change. Gold electrodeposition on HOPG followed by STM, *Langmuir* 13 (1997) 100–110.
- [17] U. Schmidt, M. Donten, J. Osteryoung, Gold electrocrystallization on carbon highly oriented pyrolytic graphite from concentrated solutions of LiCl, *J. Electrochem. Soc.* 144 (1997) 2013–2021.
- [18] B. Scharifker, G. Hills, Theoretical and experimental studies of multiple nucleation, *Electrochim. Acta* 28 (1983) 879–889.
- [19] S. Grimme, Accurate description of van der Waals complexes by density functional theory including empirical corrections, *J. Comput. Chem.* 25 (2004) 1463–1473.
- [20] M. Amft, S. Lebègue, O. Eriksson, N.V. Skorodumova, Adsorption of Cu, Ag, and Au atoms on graphene including van der Waals interactions, *J. Phys. Condens. Matter* 23 (2011) 395001–395010.